Journal of MATERIALS RESEARCH

Invited Review
DOI:10.1557/s43578-022-00796-8

BORON NITRIDE NANOTUBES

FOCUS ISSUE

# Understanding toxicity associated with boron nitride nanotubes: Review of toxicity studies, exposure assessment at manufacturing facilities, and read-across

Vamsi Kodali[1,2,a], Jenny R. Roberts[1], Eric Glassford[3], Ryan Gill[1], Sherri Friend[1], Kevin L. Dunn[3], Aaron Erdely[1,2]

[1] Health Effects Laboratory Division, National Institute for Occupational Safety and Health, 1000 Frederick Lane (MS-2015), Morgantown, WV 26508, USA
[2] Department of Physiology and Pharmacology, School of Medicine, West Virginia University, Morgantown, WV 26506, USA
[3] Division of Field Studies and Engineering, National Institute for Occupational Safety and Health, Cincinnati, OH 45226, USA
[a] Address all correspondence to this author. e-mail: ywu0@cdc.gov

Received: 1 July 2022; accepted: 12 October 2022; published online: 31 October 2022

**Boron nitride nanotubes (BNNT) are produced by many different methods leading to variances in physicochemical characteristics and impurities in the final product. These differences can alter the toxicity profile. The importance of understanding the potential pathological implications of this high aspect ratio nanomaterial is increasing as new approaches to synthesize and purify in large scale are being developed. In this review, we discuss the various factors of BNNT production that can influence its toxicity followed by summarizing the toxicity findings from in vitro and in vivo studies conducted to date, including a review of particle clearance observed with various exposure routes. To understand the risk to workers and interpret relevance of toxicological findings, exposure assessment at manufacturing facilities was discussed. Workplace exposure assessment of BNNT from two manufacturing facilities measured boron concentrations in personal breathing zones from non-detectable to 0.95 μg/m$^3$ and TEM structure counts of 0.0123 ± 0.0094 structures/cm$^3$, concentrations well below what was found with other engineered high aspect ratio nanomaterials like carbon nanotubes and nanofibers. Finally, using a purified BNNT, a "read-across" toxicity assessment was performed to demonstrate how known hazard data and physicochemical characteristics can be utilized to evaluate potential inhalation toxicity concerns.**

Research into the potential toxicity of engineered nanomaterials has been an expansive endeavor for two decades. As material size decreases from macro to micro to nano, the surface area increases leading to greater toxicity per unit mass. Categorically, engineered nanomaterials confer toxicity by solubility, biopersistence, physical shape, reactivity, etc [1, 2]. Much research has been devoted to understanding nanosized high aspect ratio materials, such as carbon nanotubes or nanofibers (CNT/F) given the known historical risk of fiber inhalation. The CNT/F research indicated mesothelioma, tumorigenesis, inflammation, translocation, and significant pulmonary pathology depending on the delivered dose and the specific type of CNT/F [3–7].

History would suggest that any high aspect ratio material with the possibility of inhalation exposure be carefully considered for potential toxicity. For reference, the National Institute for Occupational Safety and Health (NIOSH) recommended exposure limit (REL) for carbon black is 3.5 mg/m$^3$ but CNT/F is 1 μg/m$^3$, clearly indicating physical shape confers significant toxicity. Boron oxide, while causing skin, eye, and respiratory irritation, has an Occupational Safety and Health Administration (OSHA) permissible exposure limit (PEL) of 15 mg/m$^3$ (NIOSH REL is 10 mg/m$^3$), indicating boron oxide is controlled at a total dust exposure level. It is conceivable, like carbon, converting boron into a high aspect ratio nanomaterial (HARN) would affect its toxicity. Therefore, boron nitride nanotubes

(BNNT) warrant a closer inspection of its toxicity and potential for exposure.

BNNT production, which includes various synthesis methods, purification, dispersion, and its applications including in nanomedicine have been extensively reviewed [8–15]. The goal of the current review is to understand the occupational toxicity associated with BNNT. This was achieved by first listing the key characteristics of BNNT that can potentially influence its toxicity, followed by performing a literature review to summarize the important findings from studies evaluating BNNT toxicity in vitro and in vivo. Results from exposure assessment from two BNNT manufacturing facilities were provided to guide dosimetry design for future toxicity studies and provide a meaningful interpretation of the toxicological findings. Finally, we evaluated the potential toxicity of a purified BNNT utilizing physical dimension profiling and two-dimensional agglomeration in comparison to large comparative CNT/F studies as well as performing read-across using the high aspect ratio nanomaterial integrated approach to testing and assessment (HARN IATA) [16–19].

## BNNT production

BNNTs can be manufactured by several approaches [8–10] and toxicity studies have reported using BNNT manufactured by arc discharge, ball milling and annealing, self-propagation high-temperature synthesis (SHS) followed by annealing, chemical vapor deposition (CVD), high-temperature and high-pressure process (PVC/HTP), and hydrogen-assisted BNNT synthesis (HABS). Each approach is distinct and utilizes specific precursors, conditions, and equipment to promote the growth, leading to production of BNNT at various scales with unique physicochemical features including length, number of walls (diameter), defects, and process specific impurities/residuals. BNNT, similar to other HARN, are hydrophobic and can agglomerate easily due to van der Waals interactions. Aqueous dispersions are usually achieved for biocompatibility and long-term biostability by coating the BNNT. These coatings can influence the agglomeration state of BNNT and their interaction with cells and organs. All these factors can potentially affect toxicity.

As-produced BNNT manufactured by some processes can contain ~ 50 weight (wt) % high aspect ratio BNNT and ~ 50 wt% non-BNNT materials. The non-BNNT material consists of catalyst, boron, and hBN (hexagonal boron nitride) in various forms that was not consumed or partially modified in the synthesis of BNNT. The physicochemical characteristics of the impurities/residuals in the as-produced BNNT is dependent on the manufacturing processes. The as-produced BNNT by HTP and HABS predominantly contain elemental boron, amorphous boron particles encapsulated with hBN shells, as well as any of various hBN derivatives including nontubular BN phases, turbostratic BN, hBN flakes, and in case of HABS, other B–N–H intermediates [8]. Other approaches like ball milling also reported to have BNNT in relative low weight percentage and comprise of amorphous boron and boron nitride in various forms as impurity [20]. Apart from boron-based impurities, metal impurities from milling tool wear or residuals from catalysts have been reported to be present with BNNT produced by ball milling and CVD. Metal impurities have been shown to induce oxidative stress and toxicity with CNT exposures [21]. These metal impurities can be removed by acid washing the as-produced material, although consideration should be given to the level of washing and acid used, as strong acids can oxidize the surfaces and cause defects that can alter the toxicity profile [22]. The surface defects of BNNT produced by CVD were strongly dependent on tube diameter [23]. Structural defects and shortening of length have also been found in CNT with increased milling time [24]. Chemically reactive unsaturated boron atoms on the defect sites and edges can potentially lead to increased toxicity [25]. Such reactive sites at edges were also reported with other engineered and natural fiber-like materials, including SiC whiskers, asbestos, nemalite, glass, and rockwool fibers [26]. Finally, the manufacturing process dictates the length and diameter/number of walls [8], some of the primary factors affecting toxicity of high aspect ratio nanomaterials.

Given the desired material is BNNT, and impurities are known to affect the material performance, procedures to purify the final sample to create a greater ratio of BNNT to impurities have been explored [8, 20, 21, 27–35]. These approaches can remove some specific impurities and can generate unique BNNT with physicochemical characteristics dependent on the manufacturing and purification procedure employed. In terms of toxicity, one could hypothesize that an exposure to a material containing a greater number of high aspect ratio fiber-like materials compared to low aspect ratio impurity particulate would confer greater toxicity. Hence, studies of as-produced BNNT samples as well as different levels of purification with a thorough characterization of the material produced are needed to fully address any potential toxicity.

## BNNT toxicity in vitro

The BNNT used and their characteristics, cell model, toxicity endpoints, dose and time course are provided in Table 1. Apart from BNNT, a selection of toxicity studies with other BN forms have been included for comparison.

Polyethyleneimine (PEI)-coated BNNT produced via the ball milling and annealing method with Fe and Cr catalysts (~ 1.5 wt%) were evaluated in neuroblastoma cells (SH-SY5Y). These BNNT induced a dose-dependent toxicity starting at concentrations > 5 μg/ml after 24 h of treatment [36]. A time-response study at 5 μg/ml resulted in no toxicity for up to 72 h

**TABLE 1:** Studies evaluating the in vitro toxicity of BN nanotubes and nanoparticles.

| | Manufacturing process/ manufacturer | Length, diameter/distinguishable characteristic | Cell type | Toxicity endpoints | Dose/time | Lowest dose where effect was observed/ major toxicity finding | References |
|---|---|---|---|---|---|---|---|
| BNNT (Polyethyleneimine coated) | Ball Milling and Annealing method (Fe and Cr catalyst) [62] | – | Human Neuroblastoma cells (SH-SY5Y) | Cytotoxicity (MTT) | 0–10 μg/ml for 24 h | >5 μg/ml | Ciofani et al. [36] |
| BNNT (Polyethyleneimine coated) | Ball Milling and Annealing method (Fe and Cr catalyst) [62] | – | Human Neuroblastoma cells (SH-SY5Y) | Cytotoxicity (MTT, Trypan Blue), Internalization | 5 μg/ml for 24, 48 & 72 h | No Significant change. Internalization by Endocytosis | Ciofani et al. [37] |
| BNNT | CVD [23] | Diameter 20–30 nm, length up to 10 mm | Human Embryonic Kidney Cells (HEK 293) | Viability (Cell Counting), Apoptosis | 100 mg/ml for 4 days | No change in viability or Apoptosis | Chen et al. [42] |
| BNNT (Glycol chitosan coated) | SHS- Annealing [63] | 200–600 nm in length and diameter of 50 nm Shaped "bamboo- like" | Human Neuroblastoma cells (SH-SY5Y) | Cytotoxicity (MTT, WST-1), ROS | 0–100 μg/ml for 48 h | WST-1 (> 100 μg/ml) MTT (≥ 20 μg/ml) ROS (≥ 100 μg/ml) | Ciofani et al. [39] |
| BNNT (Glycol chitosan coated) | SHS- Annealing [63] | 200–600 nm in length and diameter of 50 nm. Shaped "bamboo-like" | Neuronal Cell (PC-12) | Cytotoxicity (WST-1, Live/Dead Assay) | 0–100 μg/ml for 3, 6, and 9 days | WST-1 (≥ 100 μg/ml) Live/Dead (> 50 μg/ml) | Ciofani et al. [40] |
| BNNT (Poly-L-lysine-coated) | Ball Milling and Annealing method (Fe and Cr catalyst) [62] | Hydrodynamic diameter 242 ± 92 nm | Myoblast (C2C12) | Cytotoxicity (WST-1, Trypan Blue, Live/ Dead Assay) | 0–15 μg/ml for 24, 48, and 72 h | MTT (> 15 μg/ml) Trypan Blue (No toxicity) Live/Dead (> 10 μg/ml) | Ciofani et al. [38] |
| BNNT | BNNT (Nanoamor Inc, Houston, USA) | Length 1.98 μm (range 0.43–5.8); diameter 71 nm (range 32–145 nm) (SEM) | Human Osteoblasts and Murine Macrophages (J774) | Cytotoxicity (LDH) | 1 μg/ml for 2.5 days | No Cytotoxicity | Lahiri et al. [64] |
| BNNT | CVD (with $Fe_2O_3$ Catalyst), Purification by Acid washing | Diameter 100 nm (SEM) | Human Lung Fibroblasts (MRC-5) and Tumor Cell lines (MCF-7, T98 &U87) | Cytotoxicity (MTT), Hemolysis test | 0–200 μg/ml for 48 h | IC50 = 50 μg/ml No Direct Hemolytic activity | Ferreira et al. [43] |
| BNNT (Tween 80 coated) | CVD (Boron and Magnesium Oxide as Precursors), Purified by Acid Wash [65] | Average length 10 μm, diameter 50 nm | Lung Epithelial Cells (A549), Alveolar Macrophages (RAW 264.7), Fibroblast Cells (3T3-L1), Human Embryonic Kidney Cells (HEK293) | Cytotoxicity (MTT, FMCA) | 0–20 μg/ml for 5 days. Time response 2 μg/ml for 5 days | Toxicity observed in most cells at 2 μg/ml after 48 h. Cell dependent toxicity Dose and Time dependent toxicity observed | Horvath et al. [46] |
| BNNT (APTES coated) | SHS- annealing [63] | 1 μm length,100 nm diameter. (SEM). Shaped "bamboo-like" | Mouse Fibroblasts (NIH/3T3) | Cytotoxicity (WST-1, Live/Dead, Picogreen) | 0–100 μg/ml for 24, 48, and 72 h | WST-1 (≥ 50 μg/ml). (Live/Dead (≥ 100 μg/ml) | Ciofani et al. [66] |
| BNNT (Transferrin conjugate) | – | 1 μm length,200 nm diameter (SEM). Shaped "bamboo-like" | Primary Human Umbilical Vein Endothelial Cells (HUVEC) | Cytotoxicity (WST-1, Amido Black) | 0–100 μg/ml for 24 h | ≥ 100 μg/ml | Ciofani et al. [67] |

**TABLE** 1: (continued)

| | Manufacturing process/ manufacturer | Length, diameter/distinguishable characteristic | Cell type | Toxicity endpoints | Dose/time | Lowest dose where effect was observed/ major toxicity finding | References |
|---|---|---|---|---|---|---|---|
| BNNT (Glycol chitosan coated) | SHS- annealing [63] | Diameter 125 ± 36 nm. Shaped "bamboo-like" | Primary Human Umbilical Vein Endothelial Cells (HUVEC) | Cytotoxicity (Amido Black, Trypan Blue, BrdU), Surface Expression Markers, Genotoxicity | 0–100 μg/ml for 48 h or 72 h | ≥ 100 μg/ml. No genotoxicity | Del Turco et al. [41] |
| BNNT and BNNT with various coatings | CVD | Diameter 70 nm (TEM) | Human Lung Fibroblasts (MRC-5) | Cytotoxicity (MTT)<br>ROS, Chromosomal alteration | 0–200 μg/ml for 48 h | Cytotoxicity (> 50 μg/ml)<br>ROS (≥ 100 μg/ml)<br>BNNT and one coated BNNT caused chromosomal aberration at 100 μg/ml | Ferreira et al. [44] |
| BNNT (Gum arabic coated) | CVD | Length 1.5 μm, diameter 49 ± 10 nm (TEM) | Human Neuroblastoma cells (SH-SY5Y)<br>Primary Human Umbilical Vein Endothelial Cells (HUVEC) | Cytotoxicity (WST-1, Live/Dead), Apoptosis | 0–100 μg/ml for 24, 48, and 72 h | ≥ 50 μg/ml | Ciofani et al. [48] |
| BNNT and BNNT with various coatings | CVD | Diameter 25 nm (TEM) | Lung Epithelial Cells (A549), Mammary Gland Cells), (MCF-7), Vero and Chang Liver Cells | Cytotoxicity (MTT), DNA Fragmentation | 0–1000 μg/ml for 24 h | Pristine BNNT $IC_{50}$ 250 μg/ml | Nitya et al. [68] |
| BNNT (Polydopa-mine coated) | High-Temperature/High-Pressure Process [69] | Length 1 μm, diameter 2–5 nm | Human Osteoblast Cells | Cytotoxicity (Live/Dead, Alamar blue, Picogreen) | 0–30 μg/ml for 1, 2, and 3 days | BNNT Non functionalized (≥ 1 μg/ml after 3 days)<br>Polydopamine coated BNNT (> 30 μg/ml) | Fernandez-Yague et al. [49] |
| Boron nitride nanoparticles | Momentive Performance Materials Inc (TEC020051158) | 100—250 nm (TEM) | Osteoblast Cells | Cytotoxicity (MTT)<br>ROS | 0–200 μg/ml for 1, 3, and 5 days | ≥ 200 μg/ml after 3 days, ≥ 50 μg/ml after 5 days<br>No ROS up to 50 μg/ml | Rasel et al. [60] |
| BNNT (Pectin coated) | CVD [65] | Diameter is 50 nm, interpolated length 2 μm (range 1–4 μm). Hydrodynamic diameter is 500 nm | RAW 264.7 Macrophages | Cytotoxicity (WST-1), ROS, Apoptosis, Inflammation | 0–50 μg/ml for 24 h | ≥ 50 μg/ml. No adverse effects observed up to 50 μg/ml | Rocca et al. [45] |
| BNNT-M (Dispersion media) | High-Temperature/High-Pressure Process [69] | Length 0.6–1.6 μm, diameter 13–23 nm ~ 40–50% impurities | Human peripheral blood monocyte cells (THP-1) and NLRP3 deficient THP-1 (defNLRP3 THP-1) | Cytotoxicity (LDH), ROS, Inflammation, Mechanism of Toxicity, in vitro to in vivo comparison | 0–100 μg/ml for 24 h | Toxicity (≥ 6.25 μg/ml), ROS (≥ 12.5 μg/ml), Toxicity dependent on NLRP3 and Pyroptosis dependent cell death | Kodali et al. [50] |

**TABLE** 1: (continued)

| | Manufacturing process/ manufacturer | Length, diameter/distinguishable characteristic | Cell type | Toxicity endpoints | Dose/time | Lowest dose where effect was observed/ major toxicity finding | References |
|---|---|---|---|---|---|---|---|
| Boron nitride nanosheets and nanoparticles | Ball Milling [70] | Nanosheets (1 μm & 100 nm thickness100 nm & 3 nm) Nanoparticles (100–200 nm) | Human Osteosarcoma cell line ($SaOS_2$) | Cytotoxicity (MTS) | 1 mg/ml for 7 days | BN Nanoparticles had higher toxicity than Nanosheets | Mateti et al. [25] |
| Boron nitride nanoparticles | Ball Milling | Diameter 50–190 nm, thickness 30–70 nm Density 2 g/cm$^3$. Surface area 20 m$^2$/g | Human Skin Fibroblasts (CCD-1094Sk) & Madin-Darby Canine Kidney cells (MDCK) | Cytotoxicity (MTT, SRB, Picogreen) | 0–400 μg/ml for 24 h & 48 h | ≥200 μg/ml | Kivanc et al. [59] |
| BNNT | Sigma Alrich Inc (# 802,824) | Diameter 5 nm, Surface area 100 m$^2$/g BNH (0–25%), BNN (50%), and elemental B (<25%) | CD34+ Bone Marrow Cells, Chinese Hamster Lung Fibrobalsts (V79) and Cervical Cancer (HeLa) Cells | Cytotoxicity (MTT), Genotoxicity (Comet Assay) | 0–300 μg/ml for 24 h | >300 μg/ml | Cal et al. [71] |
| BNNT (Different sizes, polyethyl-eneimine coated) | Hydrogen Catalyzed Induction Thermal Plasma Process [72] | Diameter 3.3 ± 2.4 nm. Length large 458 ± 345 nm, short 224 ± 129 nm | Human Peripheral Blood (NB4), Human Liver Epithelium (Hepg2), Human Primary Glioblastoma Epithelium (U87), Human Lung Epithelium (A549) | Cytotoxicity (WST-8, MTS, MTT) | 0–50 μg/ml for 24 h | ≥25 μg/ml. Toxicity dependent on length Cell dependent toxicity | Augustine et al. [56] |
| Boron nitride nanoparticles | Chemical Synthesis | 100—300 nm (TEM) | Human Primary Alveolar Epithelial Cells (HPAEpiC) | Cytotoxicity (MTT, NR, LDH), Microarray Analysis | 0–1280 μg/ml for 72 h | $LC_{20}$ = 125 μg/ml ≥80 μg/ml; Alteration in genes related to cell cycle, cell–cell interactions | Turkez et al. [61] |
| BNNT and purified BNNT (PEG 4000 coated) | BNNT (Sigma Aldrich Inc), Purified BNNT | BNNT (5 nm diameter, >100 m$^2$/g surface area) | Epithelial cells (CHO-K1) and Adipocytes (3T3-L1) | Cytotoxicity (WST-8) Apoptosis | 0–200 μg/ml for 48 h | Purification reduces toxicity | Lee et al. [30] |
| BNNT, hBN, 3 purified grades of BNNT (dispersion media) | Hydrogen Catalyzed Induction Thermal Plasma Process [72], Purified BNNT | Varying surface area (70 to 150 m$^2$/g for various purity grades) Pure BNNT length 1.68 μm (GSD 1.6) and diameter 0.019 μm (GSD 1.329) | Human Peripheral Blood Monocyte cells (THP-1) and NFkB Reporter THP-1 cells | Cytotoxicity (WST-1, LDH), Inflammation, Mechanism of Toxicity | 0–100 μg/ml for 24 h | BMD (10% Effect) of pure BNNT 17.2 μg/ml. Toxicity increases with purity. No toxicity in as produced BNNT. No alteration in immune function | Kodali et al. [28] |

[37]. Cellular uptake of BNNT was noted and treatment with the ATPase inhibitor (sodium azide) illustrated BNNT were internalized by energy dependent endocytosis. The same material coated with poly-l-lysine (PLL) and in a myoblasts (C2C12) cell model resulted in a similar mechanism of internalization with a significant increase in toxicity from 15 μg/ml after 72 h. At concentrations below 10 μg/ml these particulates did not induce apoptosis, necrosis, or membrane permeabilization. Exposure to 5 and 10 μg/ml up to 72 h did not induce a significant change in myoblast differentiation or tube formation [38].

BNNT with "bamboo-like" morphology synthesized by self-propagation, high-temperature synthesis (SHS) followed by annealing had a diameter range of 50–100 nm and length ranging between 200 and 600 nm [39–41]. Irrespective of coating on these BNNTs, toxicity only at the higher concentrations (> 50 or 100 μg/ml) was observed when neuroblastoma, neuronal, fibroblast and endothelial cells were exposed.

BNNT can be grown by CVD using various precursors and catalysts leading to BNNT having various physicochemical properties. Initial in vitro toxicity work in kidney cells (HEK 293) by Chen et al. [42] using BNNT manufactured by CVD using magnesium oxide as catalyst indicated no toxicity or apoptosis up to 4 days after administering the highest concentration. The BNNT had a reported diameter of 20–30 nm and length up to 10 mm. BNNT prepared via CVD using $Fe_2O_3$ as catalyst and purified by acid washing [43, 44] with a reported diameter of 70–100 nm induced dose-dependent toxicity in human lung fibroblast cells (MRC-5) with an inhibitory concentration ($IC_{50}$) of 50 μg/ml after 48 h. Similar dose–response relationships were observed in tumor cell lines. Further studies evaluating the stability and cytocompatibility of the BNNT with various functionalization found no toxicity or produced ROS up to 50 μg/ml in MRC-5 cells. At concentrations 100 μg/ml and above, polyethylene glycol and chitosan functionalization induced greater toxicity compared to BNNT alone or BNNT with glucosamine functionalization [43]. Compared to other functionalization, although not cytotoxic, BNNT alone or BNNT with glucosamine functionalization resulted in chromosomal alteration and modification in cell morphology. These differences may be due to alteration in uptake mechanism because of change in size and charge of the BNNT due to functionalization, leading to activation of distinct signaling pathways. Pectin coated BNNT with interpolated length of 1–4 μm showed no colocalization with lysosomes as well as no toxicity up to 50 μg/ml in RAW 264.7 macrophages exposed for 24 h [45]. Although pectin coated BNNT were not cytotoxic, challenge with LPS after BNNT exposure altered the transcriptional response of the macrophages. Horvath et al. [46] used BNNT produced by CVD using boron and magnesium oxide precursors, purified by acid washing, to evaluate toxicity in various cell types. The BNNT had a reported diameter of 50 nm and length of 10 μm. The BNNT in this study were found to be more potent at inducing toxicity compared to a high aspect ratio comparison CNT particle. Toxicity was induced in all cells starting at 2 μg/ml after 48 h treatment. The relative level of toxicity induced by BNNT was cell- dependent with the most toxicity in macrophages and least in renal cells. The difference in toxicity between cell types can be attributed to their function and difference in their ability to internalize the particulate. Such cell-dependent toxicity was also observed with other HARN material like CNT [47]. A follow up study [48] using similar BNNT, but shortened in length to 1.5 μm, reported reduced toxicity in neuroblastoma and endothelial cells. This decrease in toxicity with decreased length suggests, like other high aspect ratio materials, that toxicity induced by BNNT has length-dependency.

BNNT prepared using a high-temperature, and high-pressure process having diameter 2–5 nm and length less than 1 μm induced toxicity at a concentration of ≥ 1 μg/ml after 3 d of exposure in osteoblast cells [49]. When these tubes were coated with polydopamine (PD) there was no toxicity observed up to a concentration of 30 μg/ml BNNT. Change in size/charge of PD-BNNT, altered cellular recognition, or aggregation of non-functionalized BNNT (4 μm agglomerates observed in TEM) in cell culture media could be the reason for the observed difference. Kodali et al. [50] dispersed BNNT in dispersion media (DM), a biocompatible dispersant that mimics lung lining fluid [51] and used for evaluating toxicity of various fibers and 2D materials [52–55]. The dispersed BNNT had a length of 0.6–1.6 μm and a diameter of 13–23 nm. Using differentiated THP-1 wild-type and NLRP3 inflammasome-deficient macrophages, BNNT-induced toxicity, oxidative stress, and inflammation were shown to be acting in part through NLRP3 inflammasome-dependent manner. The dispersed BNNT induced lysosomal membrane damage and activated pyroptosis, a caspase-dependent pro-inflammatory form of programmed necrosis. Toxicity was significantly altered at a concentration ≥ 6.25 μg/ml and was reduced in cells deficient of NLRP3. Like the study mentioned earlier [45], macrophages pre-exposed to BNNT had an altered response when challenged with LPS. Further, a decrease in phagocyte function was observed which was dependent on NLRP3 inflammasome activation. The mechanisms of toxicity induced by BNNT was found to be similar to what has been described previously with CNT.

Augustine et al. [56] used BNNT produced by hydrogen catalyzed induction thermal plasma (HABS) having a length of 458 ± 345 nm and a shortened sample by sonication to 224 ± 129 nm. Decreasing the length eliminated the toxicity in liver, epithelial, blood, and neural cells. A study evaluating the cytotoxicity and drug encapsulating capacity of BNNT found purification of BNNTs improves several of their properties with a reduced toxicity at the higher doses [30]. The suppression in toxicity may be attributed to impurities present in the

as-produced BNNT or better dispersion of the purified BNNT potentially due to higher density of PEG coating present on the purified BNNT particles (as evident from the higher drug encapsulation and dispersion). The higher density of PEG can lead to alterations in dispersion, agglomeration, uptake mechanism, and induced cytotoxicity. Kodali et al. [28] used BNNT produced by HABS, which does not use metal catalysts, and using a sequence of purification steps, generated BNNT with different purity grades. These BNNT include, BNNT as-produced, BNNT with boron removed by gas purification, and various other non-fibrous components removed by sequential water and solvent washing. Acellular reactivity, cytotoxicity, inflammation, function, and mechanism of toxicity screening in macrophages indicated BNNT was not overtly toxic. Toxicity clustered with the purity grade of BNNT and was greatest for the samples containing a greater percent of BNNT per unit mass. The benchmark dose with 10% effect size was 17.3 μg/ml for the highest purity BNNT which had a geometric mean (geometric standard deviation) length and diameter of 1.68 (1.9) μm and 17 (1.3) nm respectively. There was a dose- and purity-dependent change in the level of inflammasome activation. Nuclear factor-κB (NF-κB) was only activated by the highest purity BNNTs at the higher concentrations and no suppression in macrophage phagocytic function was observed after challenge with bacteria.

Imbalance in oxidative stress cycle induces excessive production of reactive oxygen species (ROS) and has been implicated in pathogenesis of various disease conditions. Enhanced production of ROS has been shown to be predictive of toxicity induced by nanomaterials [57]. Nanomaterials can induce oxidative stress by intrinsic properties or indirectly as a biological response. Like cytotoxicity, reports of BNNT induced reactive oxygen species (ROS) are disparate probably due to diverse physicochemical characteristics and impurities inherent to the manufacturing process. BNNT are chemically stable and are not easily subject to oxidation; this may be altered by the presence of impurities like metal catalysts or other more reactive forms of residuals. Acellular reactivity studies by electron paramagnetic resonance (EPR) of BNNT produced by high-temperature and high-pressure [58] or HABS [28] found that the BNNT do not have active reactive sites to reach the threshold needed to induce toxicity by direct interaction. Furthermore, acellular reactivity was reduced as purity increased for BNNT samples which was inversely related to toxicity [28]. BNNT produced by high-temperature and high-pressure process induced oxidative stress in vitro [50], suggesting BNNT induced oxidative stress is part of a biological response and not from reactivity.

Boron nitride nanoparticles in various forms (e.g., hBN) are the primary residual impurity in the as-produced BNNT. Review of the toxicity of various forms of BN nanoparticles and sheets [25, 28, 59–61] indicates BN nanoparticles exposed in various cell models have reports of nontoxic, toxic at the highest concentrations, or toxicity at longer exposure duration. It is fair to assume that the toxicity of non-purified forms of BNNT consisting of these impurities will influence the toxicity conclusions induced specifically by BNNT.

## BNNT toxicity in vivo

In vivo studies evaluating the toxicity of BNNT in animal models are limited and some of the key characteristics of these studies have been captured in Table 2. The first studies evaluating in vivo toxicity of BNNT were conducted following intravenous (*i.v.*) injection to evaluate toxicity and biodistribution for drug delivery applications. The BNNT synthesized by SHS-annealing had a bamboo-like morphology with 0.5–2 μm length and a diameter of 30–100 nm [73, 74]. In vitro, this material induced toxicity only at the higher concentrations (> 50 μg/ml) and no ROS production or genotoxicity (≥ 100 μg/ml). Injection of 1 mg/kg of BNNT into New Zealand rabbits did not alter the blood cell differentials, hematological and biochemical parameters up to 72 h afterward except for small but significant change in blood platelet levels. A follow up study with 5 and 10 mg/kg single dose and 15 mg/kg repeated-dose injections found no significant alteration in hematological parameters up to 7 days after administration. In a study by Soares et al. [75], BNNT prepared by CVD having a dispersed length of 300 nm and diameter of 90 nm were radiolabeled with $^{99m}$Tc to study biodistribution in Swiss mice. The BNNT 24 h after *i.v.* injection accumulated in liver, spleen, and intestine and was eliminated by renal excretion. Intravenous injection of hexagonal boron nitride nanoparticles in Wistar rats and evaluation after 24 h showed dose-dependent effects in biochemical, hematological parameters and oxidative stress markers in various organs only at doses ≥ 1600 μg/kg. Histopathological evaluation of the liver, kidney, heart, spleen, and pancreas indicated no alteration at doses < 400 μg/kg. The damage to the tissues was dose-dependent, and at higher doses (≥ 1600 μg/kg) significant pathology was observed in all the organs evaluated [76].

Based on dustiness data of fine and nanoscale powder material [77], inhalation is expected to be a primary route of occupational exposure in workers handling BNNT. Kodali et al. [50] and Xin et al. [58] exposed high-temperature high-pressure synthesized BNNT via oropharyngeal aspiration and evaluated the pulmonary toxicity in C57BL/6 mice. At 24 h post-exposure of 40 μg BNNT, lung injury, inflammation, and induction of oxidative stress was evident from increased bronchoalveolar lavage levels of lactate dehydrogenase activity, pulmonary polymorphonuclear cell influx, loss in mitochondrial membrane potential, and augmented levels of 4-hydroxynonenal. BNNT uptake caused lysosomal destabilization, pyroptosis and NLRP3 inflammasome activation, corroborated by an increase in cathepsin B, caspase 1, and increased protein levels of IL-1β and IL-18.

**TABLE 2:** Studies evaluating the in vivo toxicity of BN nanotubes.

| | Manufacturing process/manufacturer | Length, diameter/ distinguishable characteristic | Animal model | Exposure | Toxicity endpoints | Dose/time | Lowest dose where effect was observed/ major toxicity finding | References |
|---|---|---|---|---|---|---|---|---|
| BNNT (Glycol Chitosan Coated) | SHS- annealing [63] | Length 0.5–2 μm, diameter 30–100 nm "Bamboo-like" morphology | New Zealand Rabbits | Intravenous Injection | Hemocompatibility, liver and kidney function | 1 mg/kg. 0, 2, 24 & 72 h | No toxicity observed | Ciofani et al. [73] |
| BNNT (Glycol Chitosan Coated) | CVD [23] | Length 300 nm, diameter 90 nm | Swiss Mice | Intravenous Injection | Biodistribution | 40 mg/kg. 1, 4 & 24 h | After 24 h, BNNT accumulated in the liver, spleen and gut, and eliminated via renal excretion | Soares et al. [75] |
| BNNT (Glycol Chitosan Coated) | SHS- annealing [63] | "Bamboo-like" morphology | New Zealand Rabbits | Intravenous Injection | Clearance, dose and time response | Single dose 5 or 10 mg/kg, repetitive dose 3 × 5 mg/kg. 0, 1, 3 & 7 days. 10 mg/kg 10 h | > 10 mg/kg. No significant adverse effects were found up to 7 days Circulation half-life 90 min | Ciofani et al. [74] |
| BNNT-M (Dispersion Media) | High-temperature/ high-pressure process [69] | Length 0.6–1.6 μm, diameter 13–23 nm ~40–50% impurities | Mice (C57BL/6J) | Oropharyngeal Aspiration | Lung injury, inflammation and function | 40 μg per mouse, 24 h | Pulmonary acute toxicity observed. Correlated with In Vitro endpoints | Kodali et al. [50] |
| BNNT (Dispersion Media) | High-temperature/ high-pressure process [69] | Surface Area 182.6 ± 2.4 $m^2$/g. Length 0.6–1.6 μm, diameter 13–23 nm ~40–50% impurities | Mice (C57BL/6J) | Oropharyngeal Aspiration | Lung injury, inflammation, clearance, pathology profile | 4 or 40 μg per mouse. 4 h, 1 day, 7 days, 1 mo, and 2 mo | Toxicity observed at high dose (40 μg) and not low dose (4 μg). Time dependent resolution | Xin et al. [58] |

BNNT exposure altered the cytokine response and caused a suppression in innate immune function. These finding were confirmed in vitro using THP-1 macrophages [50]. The potency of BNNT was compared to MWCNT-7, a well-studied, high aspect ratio nanomaterial that is classified as a group 2B carcinogen by the International Agency for Research on Cancer (IARC). Acute (24 h) exposure to BNNT revealed similar mechanisms of toxicity like the high aspect ratio counterpart MWCNT-7, but was less potent in inducing toxicity, inflammation, and innate immune responses.

The acute exposure BNNT study and mechanistic similarity to MWCNT-7 warranted a more detailed investigation and a longer post-exposure evaluation. Xin et al. [58] exposed the lungs to 4 and 40 μg/mouse by a single oropharyngeal aspiration. Pulmonary and systemic toxicity were investigated at 4 h, 1 day, 7 days, 1 month, and 2 months post-exposure. Extrapolating the mouse deposited dose to human equivalence, the doses of 4 and 40 μg were reported to represent, adjusting the number of days for a work year of 260 day/year, 2.4–7.3 years for the 4-μg low dose and 24.0–73.3 years for the 40-μg high dose. Lung injury and inflammation were observed with the high dose exposure and were resolved by 7 days. The lower dose did not cause any change in injury, inflammation, or cytokine secretion. Histopathological analysis confirmed that no alveolar septal thickening, hypertrophy, or hyperplasia was present in any groups. The only finding of significance was a minimal level of inflammatory cell infiltration with the high dose of exposure, which was greatest at 7 days and diminished at 2 months post-exposure. Following pulmonary exposure, systemic toxicity observed was minimal and transient. The greatest responses observed was in liver and blood cell profiles at 4 h and 1 day post-exposure in the high dose BNNT group, in part due to the bolus exposure study design. Overall, the BNNT investigated did not cause persistent in vivo toxicity in the lung or systemically up to a dose of 40 μg.

The varying purity BNNT described above in vitro [28] were evaluated in vivo. Effects were studied in male C57BL/6 mice following a single oropharyngeal exposure of 4 or 40 μg. These results have only been published in abstract form [78]. Similar to the findings in Kodali et al. [28] and Xin et al. [78], pulmonary cytotoxicity and inflammation was increased acutely and resolved over 1-month post-exposure with the greatest effect found following the administration of the high dose (40 μg) of the highest purity material. Histopathologic examination found minimal focal inflammation with microgranulomas remaining at 3 months post-exposure. Fibrosis and hyperplasia were found unremarkable.

Studies have also been conducted in several alternative animal models including *Xenopus laevis* tadpoles, *Drosophila melanogaster* and *Dugesia japonica* planarians showed BNNT to be biocompatible and not overtly toxic. In these models BNNT did not cause oxidative stress, apoptosis, DNA damage, genotoxicity and, interestingly, even positive effects like antigenotoxic potential were reported [79–81]. Studies conducted in *Caenorhabditis elegans* found soluble forms of BN nanoparticles were ten-fold more toxic compared to non-soluble forms and the toxicity threshold was 100 μg/ml and 10 μg/ml for the non-soluble and soluble forms of BN [82]. The nanosheet form of BN of varying sizes was not found to be toxic in *Bombyx mori* and other silkworm models [83, 84].

## Biopersistence and clearance of BNNT

Biopersistence of nanomaterials, which is dependent on several physicochemical properties, can be a critical factor in material-associated toxicity [85–87]. Only three studies have examined various aspects of biopersistence and clearance of BNNT following exposure in vivo, two following i.v. administration in rabbits [74] and mice [75], and one following pulmonary administration in mice [58]. As reviewed earlier, Ciofani et al. [73, 74] used rabbits to study pharmacokinetics. Animals were injected intravenously with 10 mg/kg BNNT, and blood samples were collected at five different time intervals up to 10 h post-administration. Boron concentration was measured by ICP as an indicator of BNNT in the blood. Terminal half-life was calculated by a first-order elimination model and found to be ~ 90 min. Soares et al. [75] evaluated biodistribution of radiolabeled BNNT in mice. Mice were injected *i.v.* with 40 mg/kg $^{99m}$Tc-BNNT and scintigraphic imaging was performed to quantify the radio-labeled BNNT in vivo after 19 min, 30 min, 1-, 4-, and 14-h post-injection. The labeled BNNT could be detected in liver, spleen, and gut as well as kidney and bladder within 30 min. Except for bladder, clearance was observed from all organs at 24 h, suggesting elimination through excretion. In a separate study, the authors measured biodistribution in blood, lungs, bladder, intestines, spleen, liver, and kidneys removed from animals at 10 and 30 min, and 24 h post-injection through automatic scintillation. Radioactivity was detected in all systems collected. The greatest increases 30 min post-injection were in the bladder, liver, gut, and spleen. Values decreased in most systems in a time-dependent manner and were slightly higher in bladder and liver at 24 h as compared to the other organs. The authors noted that clearance can be occurring through the kidneys by excretion, but that chitosan can be degraded by enzymes over time and, therefore, it is possible for some detachment of the radiolabel as a confounder in the results. The *i.v.* injection in rabbits and mice note low to no toxicity following exposure, which may be partly due to a high rate of elimination.

Toxicity associated with pulmonary exposure was examined by Xin et al. [58] In this study, mice that were exposed to 40 μg of a BNNT sample by oropharyngeal aspiration were examined for pulmonary clearance of BNNT at 1 day, 7 days, 1 m, and 2 m post-exposure. Lungs were digested and lung burden was

measured as boron by ICP-AES. Approximately 50% of the delivered dose measured as boron was cleared by 2 m. In this study, lung inflammation and injury that was noted in the lavage fluid and histopathology had begun to resolve over time, which correlated with clearance of the BNNT from the lung in this study. It is important to note that the BNNT sample used in this study contained ~ 50% BNNT with other boron by-products of synthesis in the sample, and that the ICP-AES analysis only examined boron as an indicator of exposure. Although toxicity was resolving to a large degree, clearance had begun to slow rapidly after 7 days. It is not clear which fraction of the BNNT sample used in this study remained in the lung up to 2 m. The fiber pathogenicity paradigm as it relates to HARN and the development of lung disease over time states that disease is dependent on dimension (fiber length and aspect ratio), durability (ability to persistent in the biological system due to lack of dissolution or breakage), and dose [88, 89], the second of which is highly dependent on the physicochemical properties of the nanomaterial. It is possible that the tube portion of the sample in this study may have differed in durability or solubility, which, in turn, may lead to fractional clearance following an exposure whereby different structures within the sample may persist longer than others. Similar to CNT [53, 90], high resolution histopathology and morphometric analysis using dark field and electron microscopy are required to shed light on the fractional clearance of different BNNT forms.

## BNNT workplace exposure assessment

Two separate BNNT production facilities were assessed for potential inhalation exposure by the NIOSH field team. These assessments included the collection of personal breathing zone and area samples for gravimetric, chemical composition, and TEM analysis. The analyses allowed for respirable and total dust exposure measurements. Additionally, surface wipe samples for chemical analysis, and the use of data logging, direct-reading instruments and workplace and work practice observations allowed for general conclusions regarding exposure. The personal air sampling was performed for the full shift range and was for ~ 7 h on average [the workers performed tasks for 48–50 min]. Personal breathing zone (PBZ) samples were collected as close as possible to the subjects breathing zone (e.g., the lapel of the lab coat). Sampling was performed in accordance with NIOSH method 9102. For wiping, pre-moistened Palintest® Dust Wipes (Palintest Inc, Kentucky, USA) were used to wipe an estimated 100 square centimeter surface. Engineering controls including local exhaust ventilation and custom-built hoods were in place during high potential exposure tasks. Based on air sampling results and other measurements and observations, the tasks most likely to have generated potential exposures included harvesting and post-harvest cleaning of the growth chambers. It is also important to note that engineering controls, work practices, and housekeeping were important factors in reducing potential worker exposures to BNNTs when workers performed various tasks.

There is no standard NIOSH or OSHA method to sample and analyze for airborne BNNT. From discussions with the NIOSH contract laboratory and NIOSH chemists, the crystalline structure of the BNNTs may not be defined during traditional chemical analysis for metal particulate using NMAM 7303 or NMAM 7302 (digestion and boron detection by ICP). Therefore, the analytical method may only measure the amorphous boron component of the aerosol and, thus, could underestimate all the boron present in the air or on a surface. Both respirable and total dust boron concentrations ranged from non-detectable to 0.95 $\mu g/m^3$. Currently the NIOSH recommended exposure limit (REL) for CNT/F is 1 $\mu g/m^3$, indicating the measured boron level, if, in fact representative of BNNT, was low but there is uncertainty with this data.

To overcome the potential limitation of boron chemical analysis, sampling results were combined with TEM analysis (modified NMAM 7402) as previously done with CNT/F [92] to identify BNNT-structures to complement the analytic method. The summary of the personal and area measurements of collected open face cassettes (meaning the values are representing the inhalable fraction) are shown in Table 3. The arithmetic mean of personal TEM BNNT concentrations was $0.0123 \pm 0.0094$ structure/$cm^3$ with a geometric mean (geometric standard deviation) of 0.0014 (7.4042). The area TEM BNNT measurements were about 2.5-fold less. It should be noted that of the combined measurements, in 62% of the samples BNNT structures were not detected. For perspective, we previously found systemic immune effects correlated to TEM structure counts of workers exposed to CNT/F [93]. Importantly, the average vales for inhalable BNNT were found to be an order of magnitude lower than CNT/F indicating significantly lower exposures in this worker population evaluated. Also, the sizes of the TEM structures were consistent with CNT/F. Most structures were in the size range of 2–10 µm with none below 1 µm. No individual/singlet BNNT's were identified during the TEM analysis, meaning, the observed structures were agglomerates (Fig. 1). For comparison with other HARN, at CNT/F facilities, 95% of the TEM structures observed were found to be agglomerates [92]. Toxicological studies evaluating potential occupational toxicity in in vitro or in vivo models should consider the agglomeration state of the test particulate.

Similar to CNT [94], based on the level of exposures measured in the BNNT manufacturing facilities, users can extrapolate their dose-dependent toxicity response to real word occupational exposures.

**TABLE 3:** Aerosol structure count characteristics at BNNT manufacturing facilities.

| | Total Samples Analyzed | Samples with ND Levels | Mean ± SE | GM (GSD) | NIOSH manual of analytical method (NMAM) [91] |
|---|---|---|---|---|---|
| Personal | | | | | |
| TEM BNNT concentration (structure/cm$^3$) | 13 | 7 | 0.0123 ± 0.0094 | 0.0014 (7.4042) | Modified NMAM 7402 with Electron energy loss spectroscopy |
| Area | | | | | |
| TEM BNNT concentration (structure/cm$^3$) | 16 | 11 | 0.0050 ± 0.0031 | 0.0007 (5.7912) | Modified NMAM 7402 with Electron energy loss spectroscopy |

*ND* not detectable, for ND, the limit of detection (1 fiber/mm$^2$) was used for calculations. *GM* geometric mean, *GSD* geometric standard deviation.

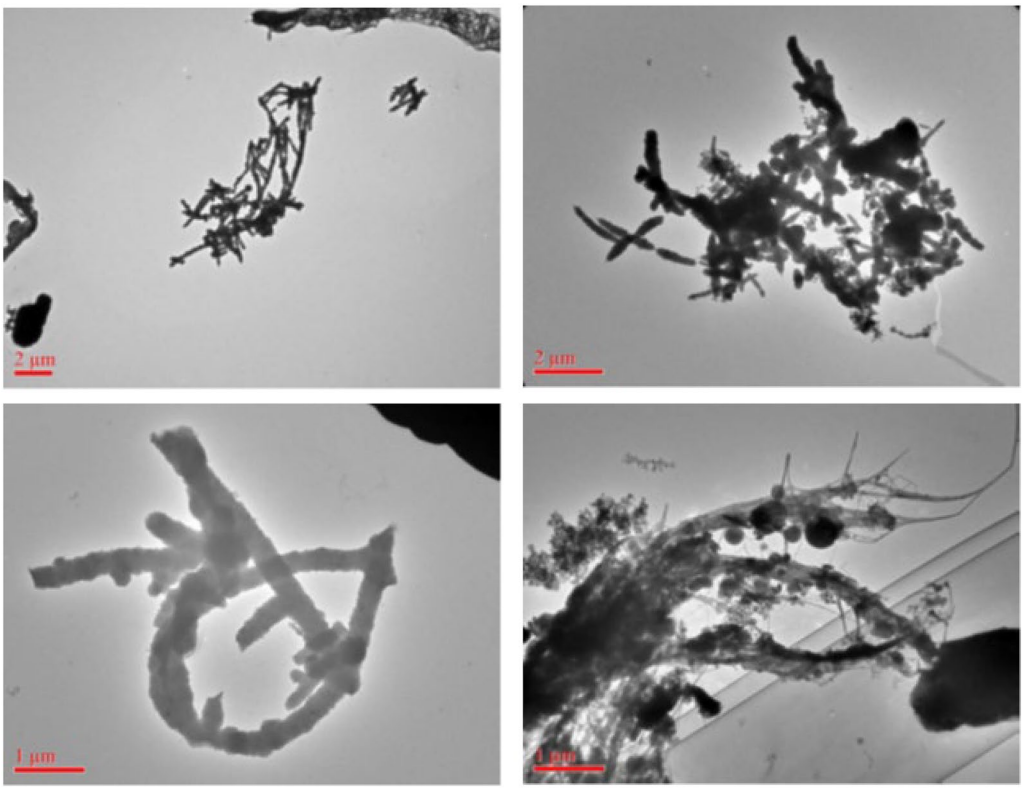


**Figure 1:** Representative images of BNNT found in the aerosols of a manufacturing facility. Electron microscopy analysis of filters collected from personal breathing zone showed agglomerates of BNNT.

## Read-across toxicity assessment of BNNT using HARN characteristics

Read-across is a process of estimating toxicity, risk or hazard posed by a substance using data on a closely related data rich surrogate. Large scale comparative studies of high aspect ratio CNT/F are being used to evaluate the unique physicochemical properties that drive distinctive aspects of toxicity [53, 54, 88, 95–98]. These outcomes are being used to allow for grouping of similar materials to facilitate read-across for predictions of toxicity [16–19, 53, 54, 99–101]. Our earlier work with CNT/F from U.S. facilities found the primary drivers of genotoxicity, inflammation, and regional pulmonary pathology were physical dimensions of length and width as well as the two-dimensional agglomeration patterns of the materials [53, 54]. In complement, an integrated approach to testing and assessment for identifying hazards posed due to inhalation of high aspect ratio nanomaterials (HARN) has been proposed by Murphy et al. [16, 19]. The HARN IATA proposes to use a tiered strategy that considers

key intrinsic material characteristics and well-defined toxicokinetic pathways or mechanisms of action elicited by a HARN to facilitate recognition of potential hazard at each tier. The tiered approach utilizes material characterization, acellular, in vitro, and in vivo models with key decision nodes identified from the fiber pathogenicity paradigm (structure–activity relationships from asbestos toxicity studies) that identify critical determinants of mesothelioma [88].

For this read-across evaluation, we used W2 BNNT that were manufactured by HABS and purified by gas purification with sequential water and solvent washing. The in vitro and in vivo toxicity of W2 BNNT has been reported previously [28, 78]. BNNT manufactured by other manufacturing processes have been reported to reach the distal lung [58]. Comparing the size and other physicochemical characteristics of W2 BNNT with previous CNT/F work [53, 102] as well as our unpublished in vivo studies of purified BNNT, the assumption would be W2 BNNT deposits in the distal lung (Fig. 2; initial decision node). As discussed in the earlier section, there was 50% clearance of boron two months post-exposure. It was not a definitive percent clearance of boron impurities compared to BNNT meaning and it is possible that the remaining 50% could be persistent BNNT. Also, BNNT are not chemically reactive, and dissolution is not expected in biological systems. Therefore, for the second decision node (Fig. 2), as not enough information is known, we consider this node as "uncertain" to be conservative. As the primary drivers of toxicity severity for CNT/F were nominal tube physical dimensions and how the material agglomerates, these same measurements were made for BNNT (Table 4; Fig. 3) using approaches described earlier [53, 54]. The BNNT materials were on average approximately 2 μm in length and 17–19 nm in diameter (Table 4). Our previous work with CNT/F indicated that binning of physical dimensions, as opposed to simply evaluating the mean values, was far superior at grouping CNT/F [54] and correlated well to toxicity outcomes evaluated [53, 54]. The HARN IATA does not consider a summary metric reporting median or mean fiber length sufficient to meet the criteria for this decision node and supports size distribution profiling with > 10% of HARN with size > 5 μm in length [19] for determining this node. Histograms representing the physical dimensions of BNNT were skewed to the left with few having larger length and diameter (Fig. 3). Only 4% of the BNNT had a length greater than 5 μm. When BNNT were dispersed using a lung lining mimetic, agglomerates were 80% spherical, meaning no one dimension was greater than 3 times another, and on average less than 1 μm in diameter (Table 4). Even the bundled agglomerates were < 2 μm in length. The third decision node (Fig. 2) is, therefore, a definitive 'no'. The fourth decision node is also a 'no' as only 3% of the measured BNNT have a diameter that exceeds 30 nm. There was no evidence or presumption of frustrated phagocytosis given the in vivo

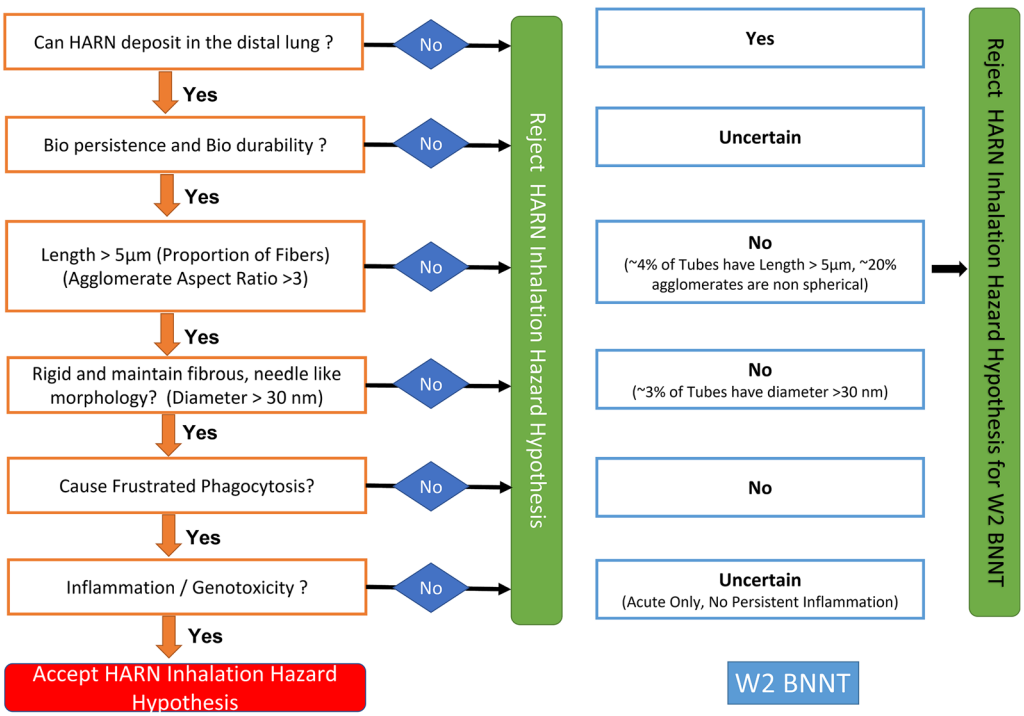


**Figure 2:** Decision nodes from HARN integrated approach to testing and assessment framework to determine potential hazard from inhalation of fiber-like material. Adapted from Murphy et al. [16]. The right side shows decision node responses to W2 BNNT.

**TABLE 4:** Characterization of W2-BNNT (a purified BNNT manufactured by HABS) dimensions dispersed in isopropanol and when agglomerated in biological dispersion media (DM).

| | Nominal tube dimensions ($N=202$) | | | | Agglomerated dimensions ($N=75$) | | | |
|---|---|---|---|---|---|---|---|---|
| | | | | | Spherical agglomerates (80%) | | Bundled agglomerates/singlets (20%) | |
| | Geometric mean (GSD) | Arithmetic mean (nm ± SE) | Median | Range | Geometric mean (GSD) | Arithmetic mean (nm ± SE) | Geometric mean (GSD) | Arithmetic mean (nm ± SE) |
| Length (μm) | 1.68 (1.94) | 2.10 ± 0.11 | 1.67 | 0.29–10.07 | | | 0.92 (1.89) | 1.13 ± 0.24 |
| Diameter (nm) | 17.84 (1.33) | 18.59 ± 0.41 | 17.90 | 9.90–55.10 | 0.59 (2.49) | 0.95 ± 0.16 | 0.21 (1.94) | 0.27 ± 0.07 |

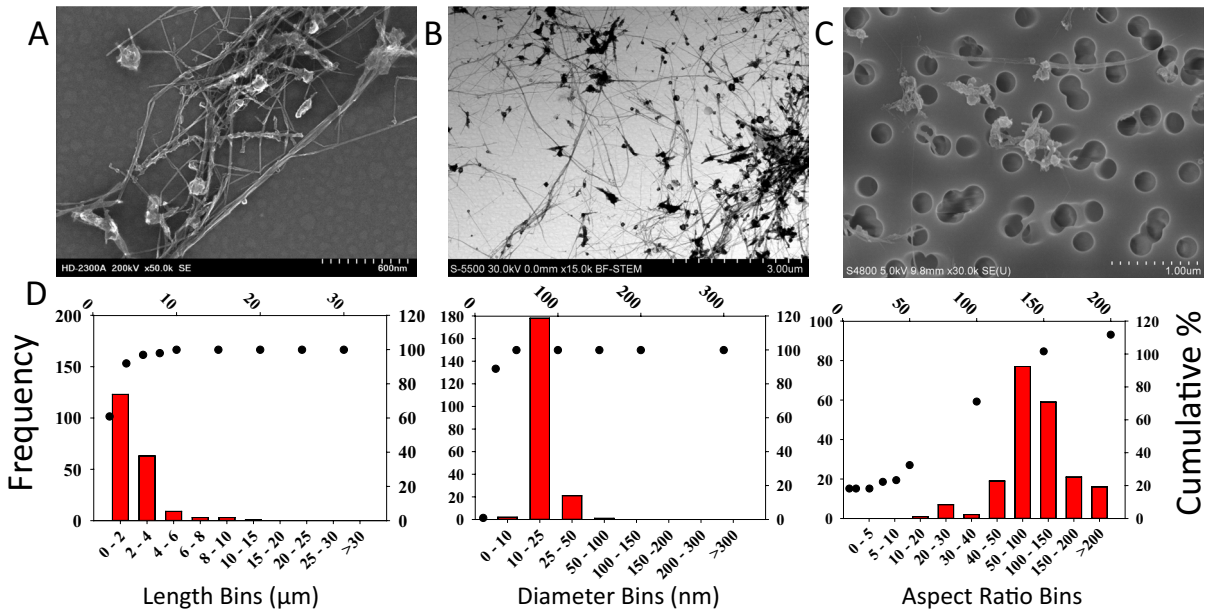


**Figure 3:** Representative field emission scanning electron microscope (A) and transmission electron microscope (B) images of W2 BNNT in isopropanol suspension used in the read-across. Representative field emission scanning electron microscope image of the aqueous dispersions of agglomerated W2 BNNT in dispersion media (C) used for the toxicity assays. Distributions of W2 BNNT length, diameter, and aspect ratio. BNNT was binned according to size along the lower x-axis with frequency on the left *y*-axis. Additionally, percentage of accumulation is graphed on the right *y*-axis with the absolute dimensions along the upper *x*-axis.

observations of collected lavage cells or the physical dimensions for decision node five. The last node is conservatively uncertain as genotoxicity was not determined, and although BNNT causes inflammation including inflammasome induction, it was not persistent.

Comparing the physical dimensions and agglomeration of W2 BNNT with previous studies of CNT/F, the materials with less severe inflammation and pathology have histograms shifted almost entirely to the left, indicating shorter lengths and diameters. Conversely, materials which conferred greater and more persistent in vivo inflammation, increased genotoxicity, bronchiolar pathology, and more severe alveolar pathology had a population of nominal tubes of greater diameter length and diameter. In relationship to our CNT/F comparative studies, the BNNT physical dimension and agglomerate pattern would suggest toxicity similarity to smaller diameter and length CNT/F and not consistent with the more toxic CNT/F [53, 54].

If we apply the HARN IATA [16–18], the BNNT samples we studied would not be consistent with the predicted development of mesothelioma. Several decision node evaluations, primarily those dependent on physical dimensions and agglomeration pattern, were not consistent with a positive outcome in the HARN IATA framework. These determinations are consistent with resolution of inflammation and minimal to no in vivo pathology by three months after BNNT exposure [58, 78].

## Summary and outlook

The in vitro studies offered some contradicting and disparate toxicity findings. These contradictions can be attributed to diverse BNNT physicochemical properties resulting from different manufacturing and purification processes. In addition, lack of a thorough physicochemical characterization, coatings, agglomeration state, study design aspects like cell type tested, exposure duration, and toxicity endpoints evaluated further make it difficult to generate a forthright conclusion and a definitive quantitative estimate for potency. The studies, however, allow us to generate some generalized conclusions.

In most in vitro studies, BNNT toxicity was observed at higher concentrations or with longer exposure times. Toxicity of BNNT was dependent on particle length in the absence of other confounding factors like metal or oxidative stress causing contaminants. The biocompatible coating and dispersion procedure (sonication) had a major influence on the toxicity as it influenced dimension and agglomeration. The cell line model used for the biocompatibility testing influenced the toxicity manifestation. Studies comparing toxicity in various cell types showed the greatest toxicity in macrophages and the least in the kidney cell line. The alteration in toxicity potency with cell models may be due to differences in uptake capacity of these cells. BNNT induced ROS as a biological response and not by directly generating radicals. Like other HARN, BNNT induced toxicity through NF-κB and NLRP3 inflammasome activation. BNNT induced cell death was based on its physicochemical properties and studies so far show it utilizes apoptosis, necrosis, and caspase-dependent pyroptosis. Inflammation and alteration in cellular function was observed with some BNNT but not all of them. In general, the manufacturing processes and purification procedures followed can affect toxicity induced by BNNT, as they modify the physicochemical properties like length, amount of high aspect ratio material, and free radical-producing impurities like residual metal catalysts.

Pulmonary BNNT exposure by oropharyngeal aspiration in mice induced acute toxicity and the mechanism of toxicity was NLRP3-dependent as observed in vitro, and with other HARN, but resolved with time. Only the higher dose of BNNT caused inflammation and lung damage. Clearance of the exposure was observed with time, inflammation was acute, and only minimal pathological alterations were observed at the highest purity and dose three months post-exposure. Intravenous injection of BNNT induced low or no toxicity in rabbits and mice. The BNNT did reach most of the systemic organs and had a high rate of clearance.

Exposure assessment at two BNNT facilities found boron concentration ranging from non-detectable to 0.95 μg/m$^3$, which, if representative solely of BNNTs, is below 1 μg/m$^3$, the NIOSH exposure limit set for CNT/F. BNNT structure count concentrations at the two manufacturing facilities were significantly lower than those measured previously at CNT/F facilities, meaning worker exposure can be adequately controlled through traditional methods such as engineering controls, work practices, and housekeeping. However, the exposure assessments indicated that harvesting of BNNT and post-harvest cleaning of growth chambers had the most likely potential for controlling exposures and should be targeted in assessment and control plans. The reduced toxicity of BNNT compared to CNT/F with an order of magnitude less structure count exposure suggests a reduced likelihood of human health effects.

Read-across of potential pulmonary hazard using previous CNT/F comparative studies and the HARN IATA predict purified BNNT (W2 BNNT manufactured by HABS) was not prone to induce remarkable pulmonary toxicity, severe long-term pathological changes, or mesothelioma. This does not mean BNNT do not pose any risk. Genotoxicity of BNNT has not been fully evaluated. A CNT/F study that evaluated genotoxicity found all nine simultaneously-tested CNT/F from U.S. facilities, despite differences in pulmonary toxicity, induced genotoxicity [54]. Ingestion and dermal exposure should also not be dismissed, as CNT/F workers had 70% incidence of dermal exposure [103, 104]. Indeed, BNNT exposure led to alteration in host-associated gut microbiota in tadpoles [80], reinforcing the need for toxicity studies with routes of exposure beyond inhalation.

In conclusion, BNNT toxicity is dependent on production process, concentration, deposited dose, study design, and purity. In comparison to more toxic CNT/F as a reference HARN, BNNT conferred less toxicity both in experimental and predictive comparisons. Additionally, initial exposure assessment evaluations indicate exposures can be controlled to levels much less than average CNT/F exposures. Future studies should focus on the more purified BNNT, especially if purification processes result in consistently extended nominal tube lengths. The comparative conclusions to other HARN may be misleading if 40% of the sample was not BNNT but impurities. Care should be taken to account for the fiber number and characteristics of the fibers when evaluating relative potency with other HARN. A robust physicochemical characterization and mechanism-based screening approach will help determine the toxicological component, the mechanism of toxicity, and offer a consensus on the potency as well as the toxicological profile of the various BNNT produced. Lastly, downstream high-volume applications like production of nanocomposites, which may use a greater % mass incorporation of BNNT compared to other HARN such as CNT/F, should be evaluated to provide any toxicity potential to workers or consumers.

## Disclaimer

The findings and conclusions in this report are those of the authors and do not necessarily represent the official position of the National Institute for Occupational Safety and Health, Centers for Disease Control and Prevention. Mention of brand name does not constitute product endorsement.

## Funding

This work was funded by the National Occupational Research Agenda (NORA) #29390G1X and National Institute for Occupational Safety and Health, Nanotechnology Research Center (NTRC) # 921043T.

## Data availability

Data reported in this manuscript can be made available upon reasonable request.

## Declarations

**Conflict of interest** The authors declare no conflict of interest.

## References

1. H. Godwin, C. Nameth, D. Avery, L.L. Bergeson, D. Bernard, E. Beryt, W. Boyes, S. Brown, A.J. Clippinger, Y. Cohen, M. Doa, C.O. Hendren, P. Holden, K. Houck, A.B. Kane, F. Klaessig, T. Kodas, R. Landsiedel, I. Lynch, T. Malloy, M.B. Miller, J. Muller, G. Oberdorster, E.J. Petersen, R.C. Pleus, P. Sayre, V. Stone, K.M. Sullivan, J. Tentschert, P. Wallis, A.E. Nel, Nanomaterial categorization for assessing risk potential to facilitate regulatory decision-making. ACS Nano. **9**(4), 3409 (2015)
2. E.D. Kuempel, V. Castranova, C.L. Geraci, P.A. Schulte, Development of risk-based nanomaterial groups for occupational exposure control. J. Nanopart. Res. **14**(9), 1029 (2012)
3. V. Castranova, P.A. Schulte, R.D. Zumwalde, Occupational nanosafety considerations for carbon nanotubes and carbon nanofibers. Acc. Chem. Res. **46**(3), 642 (2013)
4. J. Dong, Q. Ma, Advances in mechanisms and signaling pathways of carbon nanotube toxicity. Nanotoxicology **9**(5), 658 (2015)
5. T. Kasai, K. Gotoh, T. Nishizawa, T. Sasaki, T. Katagiri, Y. Umeda, T. Toya, S. Fukushima, Development of a new multi-walled carbon nanotube (MWCNT) aerosol generation and exposure system and confirmation of suitability for conducting a single-exposure inhalation study of MWCNT in rats. Nanotoxicology. **8**(2), 169 (2014)
6. G. Oberdörster, V. Castranova, B. Asgharian, P. Sayre, Inhalation exposure to carbon nanotubes (CNT) and carbon nanofibers (CNF): methodology and dosimetry. J. Toxicol. Environ. Health Part B **18**(3–4), 121 (2015)
7. R.D. Zumwalde, Occupational exposure to carbon nanotubes and nanofibers. Acc. Chem. Res. **46**(3), 642–649 (2013)
8. M.B. Jakubinek, B. Ashrafi, Y. Martinez-Rubi, J. Guan, M. Rahmat, K.S. Kim, S. Dénommée, C.T. Kingston, B. Simard, *Boron Nitride Nanotube Composites and Applications, in Nanotube Superfiber Materials* (Elsevier, Amsterdam, 2019), p.91
9. C.H. Lee, S. Bhandari, B. Tiwari, N. Yapici, D. Zhang, Y.K. Yap, Boron nitride nanotubes: recent advances in their synthesis, functionalization, and applications. Molecules **21**(7), 922 (2016)
10. T. Xu, K. Zhang, Q. Cai, N. Wang, L. Wu, Q. He, H. Wang, Y. Zhang, Y. Xie, Y. Yao, Advances in synthesis and applications of boron nitride nanotubes: a review. Chem. Eng. J. 134118 (2021)
11. E.A. Turhan, A.E. Pazarçeviren, Z. Evis, A. Tezcaner, Properties and applications of boron nitride nanotubes. Nanotechnology (2022)
12. A. Merlo, V. Mokkapati, S. Pandit, I. Mijakovic, Boron nitride nanomaterials: biocompatibility and bio-applications. Biomater. Sci. **6**(9), 2298 (2018)
13. A.B. Kakarla, I. Kong, In vitro and in vivo cytotoxicity of boron nitride nanotubes: a systematic review. Nanomaterials **12**(12), 2069 (2022)
14. M. Li, G. Huang, X. Chen, J. Yin, P. Zhang, Y. Yao, J. Shen, Y. Wu, J. Huang, Perspectives on environmental applications of hexagonal boron nitride nanomaterials. Nano Today **44**, 101486 (2022)
15. A.D.S. McWilliams, C. Martínez-Jiménez, K.R. Shumard, M. Pasquali, A.A. Martí, Dispersion and individualization of boron nitride nanotubes. J. Mater. Res. (2022)
16. F. Murphy, S. Dekkers, H. Braakhuis, L. Ma-Hock, H. Johnston, G. Janer, L. di Cristo, S. Sabella, N.R. Jacobsen, A.G. Oomen, A. Haase, T. Fernandes, V. Stone, An integrated approach to testing and assessment of high aspect ratio nanomaterials and its application for grouping based on a common mesothelioma hazard. NanoImpact **22**, 100314 (2021)
17. V. Stone, S. Gottardo, E.A.J. Bleeker, H. Braakhuis, S. Dekkers, T. Fernandes, A. Haase, N. Hunt, D. Hristozov, P. Jantunen, N. Jeliazkova, H. Johnston, L. Lamon, F. Murphy, K. Rasmussen, H. Rauscher, A.S. Jiménez, C. Svendsen, D. Spurgeon, S. Vázquez-Campos, W. Wohlleben, A.G. Oomen, A framework for grouping and read-across of nanomaterials- supporting innovation and risk assessment. Nano Today **35**, 100941 (2020)
18. F. Murphy, H.J. Johnston, S. Dekkers, E.A.J. Bleeker, A.G. Oomen, T.F. Fernandes, K. Rasmussen, P. Jantunen, H. Rauscher, N. Hunt, L. di Cristo, H.M. Braakhuis, A. Haase, D. Hristozov, W. Wohlleben, S. Sabella, V. Stone, How to formulate hypotheses and IATA to support grouping and read-across of nanoforms. ALTEX – Altern. Anim. Exp. (2022).
19. F. Murphy, N.R. Jacobsen, E. Di Ianni, H. Johnston, H. Braakhuis, W. Peijnenburg, A. Oomen, T. Fernandes, V. Stone, Grouping MWCNTs based on their similar potential to cause

pulmonary hazard after inhalation: a case-study. Particle Fibre Toxicol. **19**(1), 50 (2022)

20. J.H. Kim, T.V. Pham, J.H. Hwang, C.S. Kim, M.J. Kim, Boron nitride nanotubes: synthesis and applications. Nano Converg. **5**(1), 17 (2018)
21. S. Tsuruoka, F.R. Cassee, V. Castranova, A new approach to design safe CNTs with an understanding of redox potential. Particle Fibre Toxicol. **10**(1), 44 (2013)
22. I. Fenoglio, G. Greco, M. Tomatis, J. Muller, E. Raymundo-Piñero, F. Béguin, A. Fonseca, J.B. Nagy, D. Lison, B. Fubini, Structural defects play a major role in the acute lung toxicity of multiwall carbon nanotubes: physicochemical aspects. Chem. Res. Toxicol. **21**(9), 1690 (2008)
23. C. Tang, Y. Bando, T. Sato, K. Kurashima, A novel precursor for synthesis of pure boron nitride nanotubes. Chem. Commun. **12**, 1290 (2002)
24. B. Krause, T. Villmow, R. Boldt, M. Mende, G. Petzold, P. Pötschke, Influence of dry grinding in a ball mill on the length of multiwalled carbon nanotubes and their dispersion and percolation behaviour in melt mixed polycarbonate composites. Compos. Sci. Technol. **71**(8), 1145 (2011)
25. S. Mateti, C.S. Wong, Z. Liu, W. Yang, Y. Li, L.H. Li, Y. Chen, Biocompatibility of boron nitride nanosheets. Nano Res. **11**(1), 334 (2018)
26. B. Fubini, V. Bolis, E. Giamello, M. Volante, *Chemical Functionalities at the Broken Fibre Surface Relatable to Free Radicals Production, in Mechanisms in Fibre Carcinogenesis* (Springer, New York, 1991), p.415
27. H. Cho, S. Walker, M. Plunkett, D. Ruth, R. Iannitto, Y. Martinez Rubi, K.S. Kim, C.M. Homenick, A. Brinkmann, M. Couillard, Scalable gas-phase purification of boron nitride nanotubes by selective chlorine etching. Chem. Mater. **32**(9), 3911 (2020)
28. V.K. Kodali, K.S. Kim, J.R. Roberts, L. Bowers, M.G. Wolfarth, J. Hubczak, T. Eye, S. Friend, A.B. Stefaniak, S.S. Leonard, M. Jakubinek, A.D. Erdely, Influence of impurities from manufacturing process on the toxicity profile of boron nitride nanotubes. Small (2022).
29. S.-H. Lee, M. Kang, H. Lim, S.Y. Moon, M.J. Kim, S.G. Jang, H.J. Lee, H. Cho, S. Ahn, Purification of boron nitride nanotubes by functionalization and removal of poly (4-vinylpyridine). Appl. Surf. Sci. **555**, 149722 (2021)
30. S.-H. Lee, M.J. Kim, S. Ahn, B. Koh, Purification of boron nitride nanotubes enhances biological application properties. Int. J. Mol. Sci. **21**(4), 1529 (2020)
31. D.M. Marincel, M. Adnan, J. Ma, E.A. Bengio, M.A. Trafford, O. Kleinerman, D.V. Kosynkin, S.-H. Chu, C. Park, S.J. Hocker, Scalable purification of boron nitride nanotubes via wet thermal etching. Chem. Mater. **31**(5), 1520 (2019)
32. Y. MartinezRubi, Z.J. Jakubek, M. Chen, S. Zou, B. Simard, Quality assessment of bulk boron nitride nanotubes for advancing research, commercial, and industrial applications. ACS Appl. Nano Mater. **2**(4), 2054 (2019)
33. A.L. Tiano, C. Park, J.W. Lee, H.H. Luong, L.J. Gibbons, S.-H. Chu, S. Applin, P. Gnoffo, S. Lowther, H.J. Kim: Boron nitride nanotube: synthesis and applications, in *Nanosensors, Biosensors, and Info-Tech Sensors and Systems* 2014, (9060, International Society for Optics and Photonics, City, 2014), p. 906006.
34. C. Zhi, Y. Bando, C. Tang, S. Honda, K. Sato, H. Kuwahara, D. Golberg, Purification of boron nitride nanotubes through polymer wrapping. J. Phys. Chem. B **110**(4), 1525 (2006)
35. A.O. Maselugbo, H.B. Harrison, J.R. Alston, Boron nitride nanotubes: a review of recent progress on purification methods and techniques. J. Mater. Res. (2022)
36. G. Ciofani, V. Raffa, A. Menciassi, P. Dario, Preparation of boron nitride nanotubes aqueous dispersions for biological applications. J. Nanosci. Nanotechnol. **8**(12), 6223 (2008)
37. G. Ciofani, V. Raffa, A. Menciassi, A. Cuschieri, Cytocompatibility, interactions, and uptake of polyethyleneimine-coated boron nitride nanotubes by living cells: confirmation of their potential for biomedical applications. Biotechnol. Bioeng. **101**(4), 850 (2008)
38. G. Ciofani, L. Ricotti, S. Danti, S. Moscato, C. Nesti, D. D'Alessandro, D. Dinucci, F. Chiellini, A. Pietrabissa, M. Petrini, A. Menciassi, Investigation of interactions between poly-L-lysine-coated boron nitride nanotubes and C2C12 cells: up-take, cytocompatibility, and differentiation. Int. J. Nanomed. **5**, 285 (2010)
39. G. Ciofani, S. Danti, D. D'Alessandro, S. Moscato, A. Menciassi, Assessing cytotoxicity of boron nitride nanotubes: interference with the MTT assay. Biochem. Biophys. Res. Commun. **394**(2), 405 (2010)
40. G. Ciofani, S. Danti, D. D'Alessandro, L. Ricotti, S. Moscato, G. Bertoni, A. Falqui, S. Berrettini, M. Petrini, V. Mattoli, A. Menciassi, Enhancement of neurite outgrowth in neuronal-like cells following boron nitride nanotube-mediated stimulation. ACS Nano. **4**(10), 6267 (2010)
41. S. Del Turco, G. Ciofani, V. Cappello, M. Gemmi, T. Cervelli, C. Saponaro, S. Nitti, B. Mazzolai, G. Basta, V. Mattoli, Cytocompatibility evaluation of glycol-chitosan coated boron nitride nanotubes in human endothelial cells. Colloids Surf. B **111**, 142 (2013)
42. X. Chen, P. Wu, M. Rousseas, D. Okawa, Z. Gartner, A. Zettl, C.R. Bertozzi, Boron nitride nanotubes are noncytotoxic and can be functionalized for interaction with proteins and cells. J. Am. Chem. Soc. **131**(3), 890 (2009)
43. T.H. Ferreira, P.R.O. Silva, R.G. Santos, E.M.B. Sousa, A novel synthesis route to produce boron nitride nanotubes for bioapplications. J. Biomater. Nanobiotechnol. **2**(04), 9 (2011)
44. T.H. Ferreira, D.C.F. Soares, L.M.C. Moreira, P.R.O. da Silva, R.G. dos Santos, E.M.B. de Sousa, Boron nitride nanotubes

coated with organic hydrophilic agents: stability and cytocompatibility studies. Mater. Sci. Eng C **33**(8), 4616 (2013)

45. A. Rocca, A. Marino, S. Del Turco, V. Cappello, P. Parlanti, M. Pellegrino, D. Golberg, V. Mattoli, G. Ciofani, Pectin-coated boron nitride nanotubes: in vitro cyto-/immune-compatibility on RAW 264.7 macrophages. Biochimica et Biophysica Acta (BBA) **1860**(4), 775 (2016)
46. L. Horváth, A. Magrez, D. Golberg, C. Zhi, Y. Bando, R. Smajda, E. Horváth, L. Forró, B. Schwaller, In vitro investigation of the cellular toxicity of boron nitride nanotubes. ACS Nano. **5**(5), 3800 (2011)
47. L. Horváth, A. Magrez, L. Forró, B. Schwaller, Cell type dependence of carbon based nanomaterial toxicity. Physica Status Solidi B **247**(11–12), 3059 (2010)
48. G. Ciofani, S.D. Turco, A. Rocca, G.D. Vito, V. Cappello, M. Yamaguchi, X. Li, B. Mazzolai, G. Basta, M. Gemmi, V. Piazza, D. Golberg, V. Mattoli, Cytocompatibility evaluation of gum Arabic-coated ultra-pure boron nitride nanotubes on human cells. Nanomedicine **9**(6), 773 (2014)
49. M.A. Fernandez-Yague, A. Larrañaga, O. Gladkovskaya, A. Stanley, G. Tadayyon, Y. Guo, J.-R. Sarasua, S.A. Tofail, D.I. Zeugolis, A. Pandit, Effects of polydopamine functionalization on boron nitride nanotube dispersion and cytocompatibility. Bioconjugate Chem. **26**(10), 2025 (2015)
50. V.K. Kodali, J.R. Roberts, M. Shoeb, M.G. Wolfarth, L. Bishop, T. Eye, M. Barger, K.A. Roach, S. Friend, D. Schwegler-Berry, B.T. Chen, A. Stefaniak, K.C. Jordan, R.R. Whitney, D.W. Porter, A.D. Erdely, Acute in vitro and in vivo toxicity of a commercial grade boron nitride nanotube mixture. Nanotoxicology **11**(8), 1040 (2017)
51. D. Porter, K. Sriram, M. Wolfarth, A. Jefferson, D. Schwegler-Berry, M.E. Andrew, V. Castranova, A biocompatible medium for nanoparticle dispersion. Nanotoxicology **2**(3), 144 (2008)
52. L. Bishop, L. Cena, M. Orandle, N. Yanamala, M.M. Dahm, M.E. Birch, D.E. Evans, V.K. Kodali, T. Eye, L. Battelli, P.C. Zeidler-Erdely, G. Casuccio, K. Bunker, J.S. Lupoi, T.L. Lersch, A.B. Stefaniak, T. Sager, A. Afshari, D. Schwegler-Berry, S. Friend, J. Kang, K.J. Siegrist, C.A. Mitchell, D.T. Lowry, M.L. Kashon, R.R. Mercer, C.L. Geraci, M.K. Schubauer-Berigan, L.M. Sargent, A. Erdely, In vivo toxicity assessment of occupational components of the carbon nanotube life cycle to provide context to potential health effects. ACS Nano. **11**(9), 8849 (2017)
53. K. Fraser, A. Hubbs, N. Yanamala, R.R. Mercer, T.A. Stueckle, J. Jensen, T. Eye, L. Battelli, S. Clingerman, K. Fluharty, T. Dodd, G. Casuccio, K. Bunker, T.L. Lersch, M.L. Kashon, M. Orandle, M. Dahm, M.K. Schubauer-Berigan, V. Kodali, A. Erdely, Histopathology of the broad class of carbon nanotubes and nanofibers used or produced in U.S. facilities in a murine model. Particle Fibre Toxicol. **18**(1), 47 (2021)
54. K. Fraser, V. Kodali, N. Yanamala, M.E. Birch, L. Cena, G. Casuccio, K. Bunker, T.L. Lersch, D.E. Evans, A. Stefaniak, M.A. Hammer, M.L. Kashon, T. Boots, T. Eye, J. Hubczak, S.A. Friend, M. Dahm, M.K. Schubauer-Berigan, K. Siegrist, D. Lowry, A.K. Bauer, L.M. Sargent, A. Erdely, Physicochemical characterization and genotoxicity of the broad class of carbon nanotubes and nanofibers used or produced in U.S. facilities. Particle Fibre Toxicol. **17**(1), 62 (2020)
55. J.R. Roberts, R.R. Mercer, A.B. Stefaniak, M.S. Seehra, U.K. Geddam, I.S. Chaudhuri, A. Kyrlidis, V.K. Kodali, T. Sager, A. Kenyon, S.A. Bilgesu, T. Eye, J.F. Scabilloni, S.S. Leonard, N.R. Fix, D. Schwegler-Berry, B.Y. Farris, M.G. Wolfarth, D.W. Porter, V. Castranova, A. Erdely, Evaluation of pulmonary and systemic toxicity following lung exposure to graphite nanoplates: a member of the graphene-based nanomaterial family. Particle Fibre Toxicol. **13**(1), 34 (2016)
56. J. Augustine, T. Cheung, V. Gies, J. Boughton, M. Chen, Z.J. Jakubek, S. Walker, Y. Martinez-Rubi, B. Simard, S. Zou, Assessing size-dependent cytotoxicity of boron nitride nanotubes using a novel cardiomyocyte AFM assay. Nanoscale Adv. **1**(5), 1914 (2019)
57. V. Kodali, B.D. Thrall, Oxidative stress and nanomaterial-cellular interactions, in *Studies on Experimental Toxicology and Pharmacology*. ed. by S.M. Roberts, J.P. Kehrer, L.-O. Klotz (Springer, New York, 2015), p.347
58. X. Xin, M. Barger, K.A. Roach, L. Bowers, A.B. Stefaniak, V. Kodali, E. Glassford, K.L. Dunn, K.H. Dunn, M. Wolfarth, S. Friend, S.S. Leonard, M. Kashon, D.W. Porter, A. Erdely, J.R. Roberts, Toxicity evaluation following pulmonary exposure to an as-manufactured dispersed boron nitride nanotube (BNNT) material in vivo. NanoImpact. **19**, 100235 (2020)
59. M. Kıvanç, B. Barutca, A.T. Koparal, Y. Göncü, S.H. Bostancı, N. Ay, Effects of hexagonal boron nitride nanoparticles on antimicrobial and antibiofilm activities, cell viability. Mater. Sci. Eng. C **91**, 115 (2018)
60. M.A.I. Rasel, T. Li, T.D. Nguyen, S. Singh, Y. Zhou, Y. Xiao, Y. Gu, Biophysical response of living cells to boron nitride nanoparticles: uptake mechanism and bio-mechanical characterization. J. Nanopart. Res. **17**(11), 441 (2015)
61. H. Türkez, M.E. Arslan, E. Sönmez, M. Açikyildiz, A. Tatar, F. Geyikoğlu, Synthesis, characterization and cytotoxicity of boron nitride nanoparticles: emphasis on toxicogenomics. Cytotechnology **71**(1), 351 (2019)
62. J. Yu, Y. Chen, R. Wuhrer, Z. Liu, S.P. Ringer, In situ formation of BN nanotubes during nitriding reactions. Chem. Mater. **17**(20), 5172 (2005)
63. J. Wang, Y. Gu, L. Zhang, G. Zhao, Z. Zhang, Synthesis of boron nitride nanotubes by self-propagation high-temperature synthesis and annealing method. J. Nanomater. **2010**, 540456 (2010)
64. D. Lahiri, F. Rouzaud, T. Richard, A.K. Keshri, S.R. Bakshi, L. Kos, A. Agarwal, Boron nitride nanotube reinforced polylactide–polycaprolactone copolymer composite: mechanical

properties and cytocompatibility with osteoblasts and macrophages in vitro. Acta Biomater. **6**(9), 3524 (2010)

65. C. Zhi, Y. Bando, C. Tan, D. Golberg, Effective precursor for high yield synthesis of pure BN nanotubes. Solid State Commun. **135**(1), 67 (2005)
66. G. Ciofani, G.G. Genchi, I. Liakos, A. Athanassiou, D. Dinucci, F. Chiellini, V. Mattoli, A simple approach to covalent functionalization of boron nitride nanotubes. J. Colloid Interface Sci. **374**(1), 308 (2012)
67. G. Ciofani, S. Del Turco, G.G. Genchi, D. D'Alessandro, G. Basta, V. Mattoli, Transferrin-conjugated boron nitride nanotubes: protein grafting, characterization, and interaction with human endothelial cells. Int. J. Pharm. **436**(1), 444 (2012)
68. J.S.M. Nithya, A. Pandurangan, Aqueous dispersion of polymer coated boron nitride nanotubes and their antibacterial and cytotoxicity studies. RSC Adv. **4**(60), 32031 (2014)
69. M.W. Smith, K.C. Jordan, C. Park, J.-W. Kim, P.T. Lillehei, R. Crooks, J.S. Harrison, Very long single- and few-walled boron nitride nanotubes via the pressurized vapor/condenser method. Nanotechnology **20**(50), 505604 (2009)
70. T. Xing, S. Mateti, L.H. Li, F. Ma, A. Du, Y. Gogotsi, Y. Chen, Gas protection of two-dimensional nanomaterials from high-energy impacts. Sci. Rep. **6**(1), 35532 (2016)
71. T. Çal, Ü.Ü. Bucurgat, In vitro investigation of the effects of boron nitride nanotubes and curcumin on DNA damage. DARU J. Pharm Sci. **27**(1), 203 (2019)
72. K.S. Kim, C.T. Kingston, A. Hrdina, M.B. Jakubinek, J. Guan, M. Plunkett, B. Simard, Hydrogen-catalyzed, pilot-scale production of small-diameter boron nitride nanotubes and their macroscopic assemblies. ACS Nano **8**(6), 6211 (2014)
73. G. Ciofani, S. Danti, G.G. Genchi, D. D'Alessandro, J.-L. Pellequer, M. Odorico, V. Mattoli, M. Giorgi, Pilot in vivo toxicological investigation of boron nitride nanotubes. Int. J. Nanomed. **7**, 19 (2012)
74. G. Ciofani, S. Danti, S. Nitti, B. Mazzolai, V. Mattoli, M. Giorgi, Biocompatibility of boron nitride nanotubes: an up-date of in vivo toxicological investigation. Int. J. Pharm. **444**(1–2), 85 (2013)
75. D.C.F. Soares, T.H. Ferreira, C.D.A. Ferreira, V.N. Cardoso, E.M.B. de Sousa, Boron nitride nanotubes radiolabeled with 99mTc: preparation, physicochemical characterization, biodistribution study, and scintigraphic imaging in Swiss mice. Int. J. Pharm. **423**(2), 489 (2012)
76. F. Kar, C. Hacıoğlu, Y. Göncü, İ Söğüt, H. Şenturk, D. Burukoğlu Dönmez, G. Kanbak, N. Ay, In vivo assessment of the effect of hexagonal boron nitride nanoparticles on biochemical, histopathological, oxidant and antioxidant status. J. Clust. Sci. **32**(2), 517 (2021)
77. D.E. Evans, L.A. Turkevich, C.T. Roettgers, G.J. Deye, P.A. Baron, Dustiness of fine and nanoscale powders. Ann. Occup. Hyg. **57**(2), 261 (2012)
78. X. Xin, M. Barger, K.A. Roach, L. Bowers, V. Kodali, K.S. Jakubinek Michael Kim, D. S, M. Wolfarth, S. Friend, S.S. Leonard, M. Kashon, D.W. Porter, A. Erdely, J.R. Roberts, In vivo lung toxicity associated with boron nitride nanotubes with different purities., in *Society of Toxiclogy Annual Meeting*, (Toxicologist, City, 2020), p. 277
79. E. Demir, R. Marcos, Antigenotoxic potential of boron nitride nanotubes. Nanotoxicology **12**(8), 868 (2018)
80. L. Evariste, E. Flahaut, C. Baratange, M. Barret, F. Mouchet, E. Pinelli, A.M. Galibert, B. Soula, L. Gauthier, Ecotoxicological assessment of commercial boron nitride nanotubes toward Xenopus laevis tadpoles and host-associated gut microbiota. Nanotoxicology **15**(1), 35 (2021)
81. A. Salvetti, L. Rossi, P. Iacopetti, X. Li, S. Nitti, T. Pellegrino, V. Mattoli, D. Golberg, G. Ciofani, In vivo biocompatibility of boron nitride nanotubes: effects on stem cell biology and tissue regeneration in planarians. Nanomedicine **10**(12), 1911 (2015)
82. N. Wang, H. Wang, C. Tang, S. Lei, W. Shen, C. Wang, G. Wang, Z. Wang, L. Wang, Toxicity evaluation of boron nitride nanospheres and water-soluble boron nitride in *Caenorhabditis elegans*. Int. J. Nanomed. **12**, 5941 (2017)
83. V. Andoh, H. Liu, L. Ma, In vivo toxicity evaluation of boron nitride nanosheets with different sizes by silkworm model. Beilstein Arch. **2021**(1), 8 (2021)
84. L. Ma, V. Andoh, M.O. Adjei, H. Liu, Z. Shen, L. Li, J. Song, W. Zhao, G. Wu, In vivo toxicity evaluation of boron nitride nanosheets in Bombyx mori silkworm model. Chemosphere **247**, 125877 (2020)
85. G. Oberdörster, T.A.J. Kuhlbusch, In vivo effects: methodologies and biokinetics of inhaled nanomaterials. NanoImpact **10**, 38 (2018)
86. W. Utembe, K. Potgieter, A.B. Stefaniak, M. Gulumian, Dissolution and biodurability: important parameters needed for risk assessment of nanomaterials. Particle Fibre Toxicol. **12**(1), 11 (2015)
87. G. Oberdörster, A. Maynard, K. Donaldson, V. Castranova, J. Fitzpatrick, K. Ausman, J. Carter, B. Karn, W. Kreyling, D. Lai, Principles for characterizing the potential human health effects from exposure to nanomaterials: elements of a screening strategy. Particle Fibre Toxicol. **2**(1), 1 (2005)
88. K. Donaldson, F.A. Murphy, R. Duffin, C.A. Poland, Asbestos, carbon nanotubes and the pleural mesothelium: a review of the hypothesis regarding the role of long fibre retention in the parietal pleura, inflammation and mesothelioma. Particle Fibre Toxicol. **7**(1), 5 (2010)
89. C.A. Poland, R. Duffin, K. Donaldson, High aspect ratio nanoparticles and the fibre pathogenicity paradigm. Nanotoxicity **61** (2009)
90. R.R. Mercer, A.F. Hubbs, J.F. Scabilloni, L. Wang, L.A. Battelli, S. Friend, V. Castranova, D.W. Porter, Pulmonary fibrotic response

to aspiration of multi-walled carbon nanotubes. Particle Fibre Toxicol. **8**(1), 21 (2011)
91. R. Andrews, P.F. O'Connor, NIOSH manual of analytical methods (NMAM), edited by N. I. F. O. S. A. H. (NIOSH), City, 2020).
92. M.M. Dahm, M.K. Schubauer-Berigan, D.E. Evans, M.E. Birch, S. Bertke, J.D. Beard, A. Erdely, J.E. Fernback, R.R. Mercer, S.A. Grinshpun, Exposure assessments for a cross-sectional epidemiologic study of US carbon nanotube and nanofiber workers. Int. J. Hyg. Environ. Health **221**(3), 429 (2018)
93. M.K. Schubauer-Berigan, M.M. Dahm, C.A. Toennis, D.L. Sammons, T. Eye, V. Kodali, P.C. Zeidler-Erdely, A. Erdely, Association of occupational exposures with ex vivo functional immune response in workers handling carbon nanotubes and nanofibers. Nanotoxicology **14**(3), 404 (2020)
94. A. Erdely, M. Dahm, B.T. Chen, P.C. Zeidler-Erdely, J.E. Fernback, M.E. Birch, D.E. Evans, M.L. Kashon, J.A. Deddens, T. Hulderman, S.A. Bilgesu, L. Battelli, D. Schwegler-Berry, H.D. Leonard, W. McKinney, D.G. Frazer, J.M. Antonini, D.W. Porter, V. Castranova, M.K. Schubauer-Berigan, Carbon nanotube dosimetry: from workplace exposure assessment to inhalation toxicology. Particle Fibre Toxicol. **10**(1), 53 (2013)
95. P. Jackson, K. Kling, K.A. Jensen, P.A. Clausen, A.M. Madsen, H. Wallin, U. Vogel, Characterization of genotoxic response to 15 multiwalled carbon nanotubes with variable physicochemical properties including surface functionalizations in the FE 1-Muta (TM) mouse lung epithelial cell line. Environ. Mol. Mutagen. **56**(2), 183 (2015)
96. H. Nagai, Y. Okazaki, S.H. Chew, N. Misawa, Y. Yamashita, S. Akatsuka, T. Ishihara, K. Yamashita, Y. Yoshikawa, H. Yasui, L. Jiang, H. Ohara, T. Takahashi, G. Ichihara, K. Kostarelos, Y. Miyata, H. Shinohara, S. Toyokuni, Diameter and rigidity of multiwalled carbon nanotubes are critical factors in mesothelial injury and carcinogenesis. Proc. Natl. Acad. Sci. **108**(49), E1330 (2011)
97. S.S. Poulsen, P. Jackson, K. Kling, K.B. Knudsen, V. Skaug, Z.O. Kyjovska, B.L. Thomsen, P.A. Clausen, R. Atluri, T. Berthing, S. Bengtson, H. Wolff, K.A. Jensen, H. Wallin, U. Vogel, Multi-walled carbon nanotube physicochemical properties predict pulmonary inflammation and genotoxicity. Nanotoxicology **10**(9), 1263 (2016)
98. S.S. Poulsen, K.B. Knudsen, P. Jackson, I.E.K. Weydahl, A.T. Saber, H. Wallin, U. Vogel, Multi-walled carbon nanotube-physicochemical properties predict the systemic acute phase response following pulmonary exposure in mice. PLoS ONE **12**(4), e0174167 (2017)
99. N. Jeliazkova, E. Bleeker, R. Cross, A. Haase, G. Janer, W. Peijnenburg, M. Pink, H. Rauscher, C. Svendsen, G. Tsiliki, A. Zabeo, D. Hristozov, V. Stone, W. Wohlleben, How can we justify grouping of nanoforms for hazard assessment? Concepts and tools to quantify similarity. NanoImpact **25**, 100366 (2022)
100. G. Tsiliki, D. Ag Seleci, A. Zabeo, G. Basei, D. Hristozov, N. Jeliazkova, M. Boyles, F. Murphy, W. Peijnenburg, W. Wohlleben, V. Stone, Bayesian based similarity assessment of nanomaterials to inform grouping. NanoImpact **25**, 100389 (2022)
101. R. Verdon, V. Stone, F. Murphy, E. Christopher, H. Johnston, S. Doak, U. Vogel, A. Haase, A. Kermanizadeh, The application of existing genotoxicity methodologies for grouping of nanomaterials: towards an integrated approach to testing and assessment. Particle Fibre Toxicol. **19**(1), 1–9 (2022)
102. R.R. Mercer, J.F. Scabilloni, A.F. Hubbs, L.A. Battelli, W. McKinney, S. Friend, M.G. Wolfarth, M. Andrew, V. Castranova, D.W. Porter, Distribution and fibrotic response following inhalation exposure to multi-walled carbon nanotubes. Particle Fibre Toxicol. **10**(1), 33 (2013)
103. M.M. Dahm, D.E. Evans, M.K. Schubauer-Berigan, M.E. Birch, J.E. Fernback, Occupational exposure assessment in carbon nanotube and nanofiber primary and secondary manufacturers. Ann. Occup. Hyg. **56**(5), 542 (2012)
104. M.M. Dahm, M.K. Schubauer-Berigan, D.E. Evans, M.E. Birch, J.E. Fernback, J.A. Deddens, Carbon nanotube and nanofiber exposure assessments: an analysis of 14 site visits. Ann. Occup. Hyg. **59**(6), 705 (2015)